ECERTA PROJECT

Computational Aeroelasticity based on Bifurcation Theory

Sebastian Timme

Kenneth J. Badcock

UNIVERSITY OF LIVERPOOL

Overview

- Motivation
- Bifurcation approach and BIFOR Solver
- Oscillatory Instability Boundary
- Conclusion

Motivation

Motivation

- Benchmark case of Isogai, NACA 64A010 aerofoil at zero angle of attack

Time response to initial disturbance

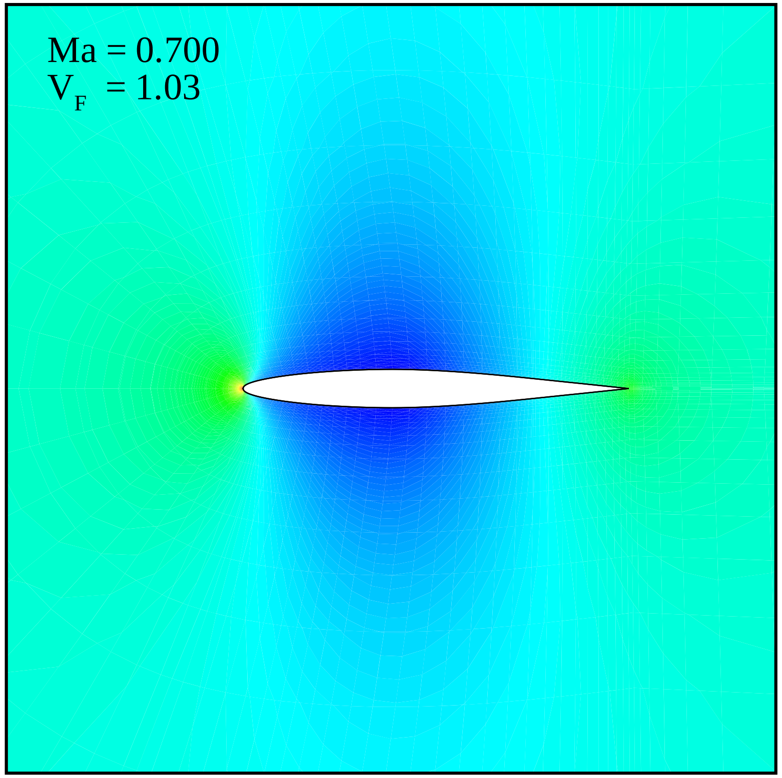

stable (Ma=0.700, V_F=1.03)

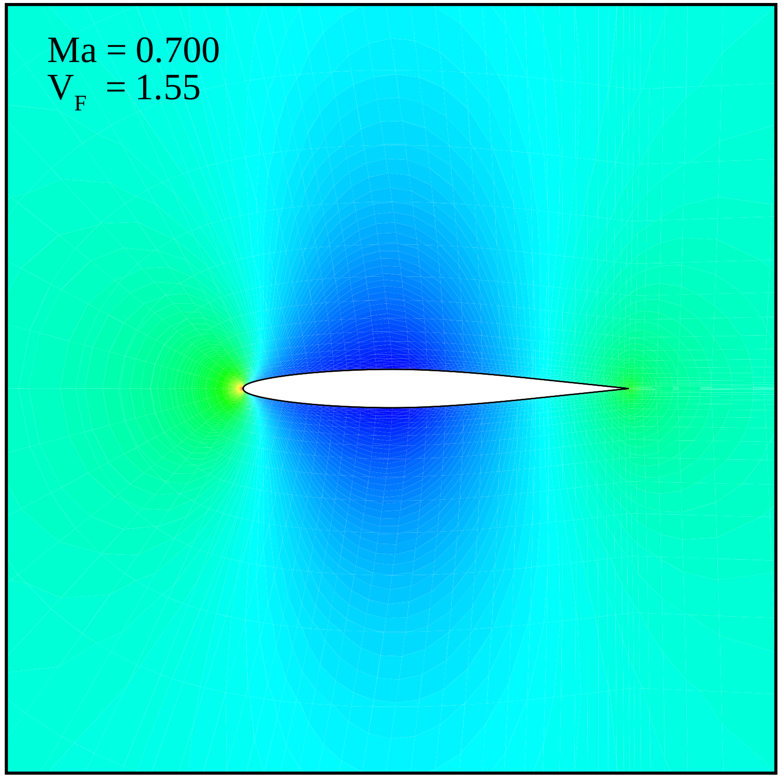

unstable (Ma=0.700, V_F=1.55)

[Isogai, AIAA Journal 18 (1981) no. 9, pp. 1240–1242]

Motivation

- Benchmark case of Isogai, NACA 64A010 aerofoil at zero angle of attack

Time response to initial disturbance

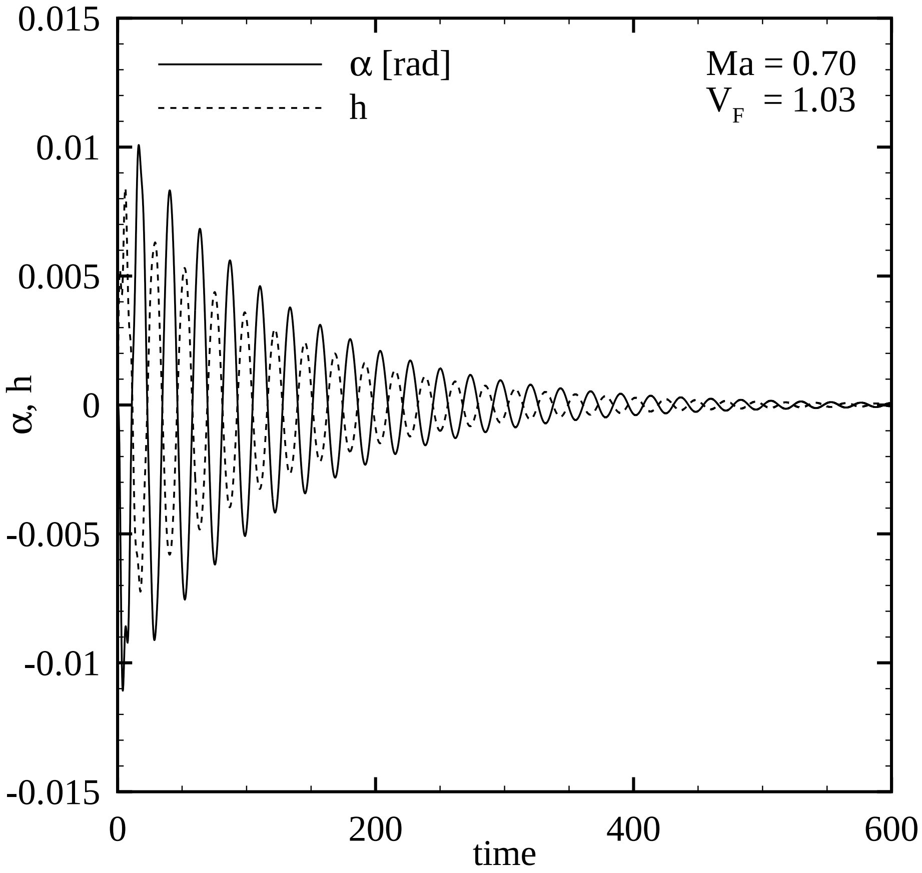

stable (Ma=0.700, V_F=1.03)

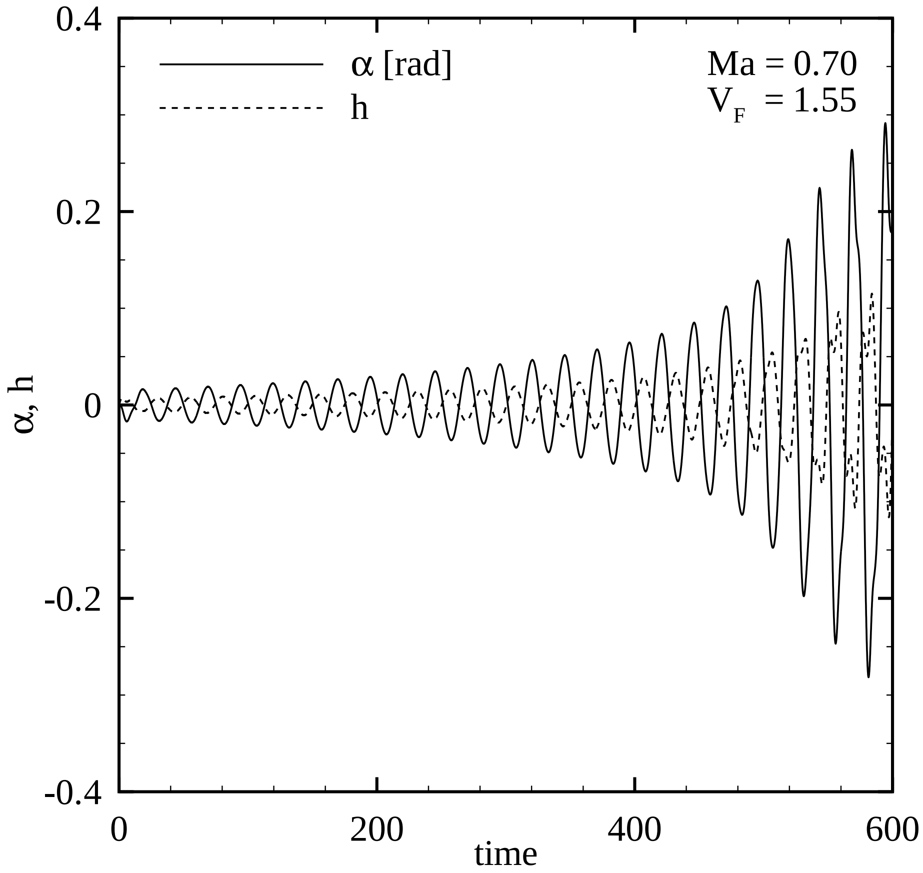

unstable (Ma=0.700, V_F=1.55)

[Isogai, AIAA Journal 18 (1981) no. 9, pp. 1240–1242]

- Benchmark case of Isogai, NACA 64A010 aerofoil at zero angle of attack

Time response to initial disturbance

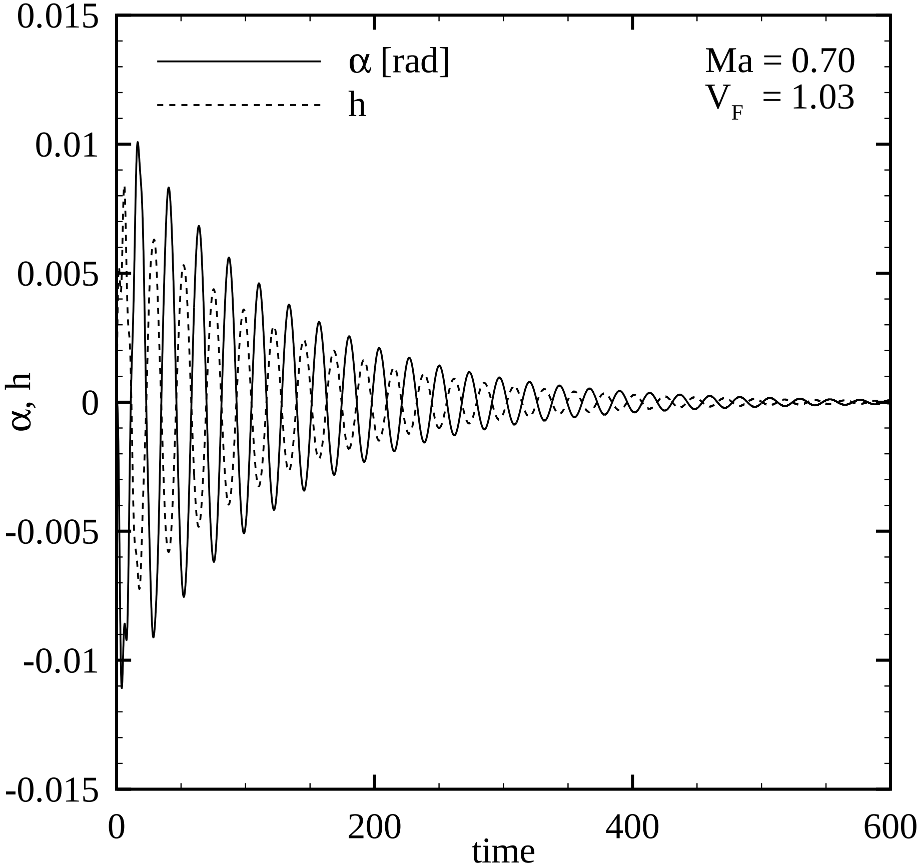

stable (Ma=0.700, V_F=1.03)

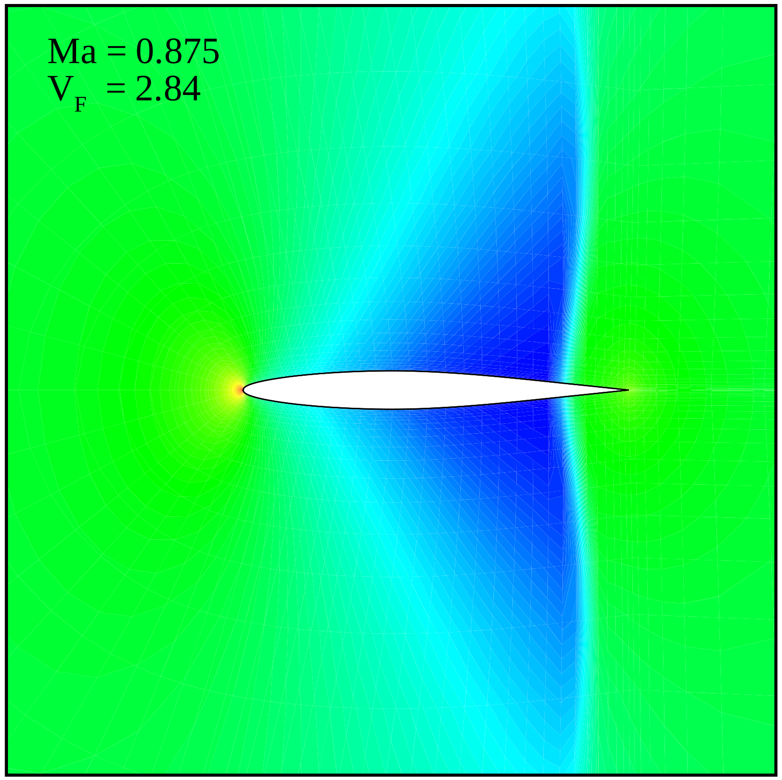

unstable (Ma=0.875, V_F=2.84)

[Isogai, AIAA Journal 18 (1981) no. 9, pp. 1240–1242]

Motivation

- Benchmark case of Isogai, NACA 64A010 aerofoil at zero angle of attack

Time response to initial disturbance

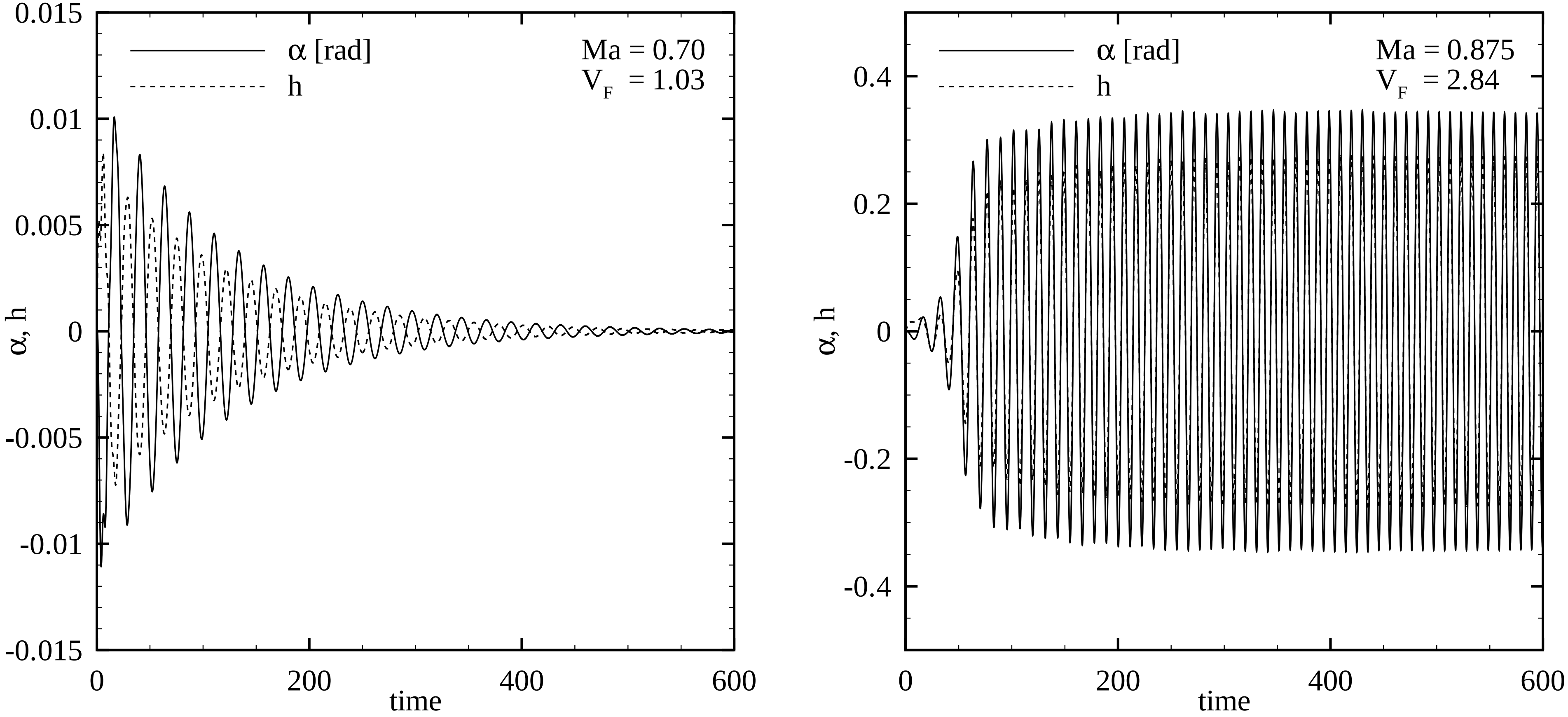

stable (Ma=0.700, V_F=1.03) unstable (Ma=0.875, V_F=2.84)

[Isogai, AIAA Journal 18 (1981) no. 9, pp. 1240–1242]

BIFOR Solver

BIFOR Solver

- Coupled full–order fluid/structure solver
- Three main parts:
  - Steady state solver (Euler, Euler/BL and Full Potential)
  - Eigenvalue solver (shifted inverse power method algorithm, Newton eigenvalue solver)
  - Unsteady time–accurate solver

BIFOR Solver

- Coupled full–order fluid/structure solver
- Three main parts
- Steady state solver (Euler):
  - Implicit time marching
  - Osher's approximate Riemann solver
  - MUSCL variable extrapolation and van Albada's limiter
  - Preconditioned Krylov subspace method
  - Applied within pseudo–time iterations in unsteady calculations

  [Badcock et al, Progress in Aerospace Sciences 36 (2000), pp. 351–392]

BIFOR Solver

- Coupled full–order fluid/structure solver
- Three main parts
- Steady state solver
- Consider coupled fluid–structure system $\Rightarrow \dfrac{d\boldsymbol{w}}{dt} = \boldsymbol{R}(\boldsymbol{w}(\mu), \mu)$
- Equilibrium $\boldsymbol{w}_0$ given by $\Rightarrow \boldsymbol{R}(\boldsymbol{w}_0(\mu), \mu) = 0$
  - Shock nonlinearity (location and strength) defined in steady flow field

BIFOR Solver

UNIVERSITY OF LIVERPOOL

- Coupled full–order fluid/structure solver
- Three main parts
- Steady state solver
- Consider coupled fluid–structure system $\Rightarrow$ $\dfrac{d\boldsymbol{w}}{dt} = \boldsymbol{R}(\boldsymbol{w}(\mu), \mu)$
- Equilibrium $\boldsymbol{w}_0$ given by $\Rightarrow$ $\boldsymbol{R}(\boldsymbol{w}_0(\mu), \mu) = 0$
- Stability determined by eigenvalues $\lambda_j = \gamma_j \pm i\omega_j$ of Jacobian $\Rightarrow$ $A(\boldsymbol{w}_0, \mu) = \dfrac{\partial \boldsymbol{R}}{\partial \boldsymbol{w}}$
  - Small number of eigenvalues associated with loss of stability
  - Dynamics of system dominated by evolution of these critical modes

BIFOR Solver

- Coupled full–order fluid/structure solver
- Three main parts
- Steady state solver
- Consider coupled fluid–structure system $\Rightarrow \dfrac{d\boldsymbol{w}}{dt} = \boldsymbol{R}(\boldsymbol{w}(\mu), \mu)$
- Equilibrium $\boldsymbol{w}_0$ given by $\Rightarrow \boldsymbol{R}(\boldsymbol{w}_0(\mu), \mu) = 0$
- Stability determined by eigenvalues $\lambda_j = \gamma_j \pm i\omega_j$ of Jacobian $\Rightarrow A(\boldsymbol{w}_0, \mu) = \dfrac{\partial \boldsymbol{R}}{\partial \boldsymbol{w}}$
- Extended eigenvalue problem $\Rightarrow \boldsymbol{R}_{EV}(\lambda, \boldsymbol{p}) = \begin{bmatrix} (A - \lambda I)\,\boldsymbol{p} \\ \boldsymbol{q}_s^T \boldsymbol{p} - i \end{bmatrix} = 0$

BIFOR Solver

- Coupled full–order fluid/structure solver
- Three main parts
- Steady state solver
- Consider coupled fluid–structure system $\Rightarrow$ $\dfrac{d\boldsymbol{w}}{dt} = \boldsymbol{R}\big(\boldsymbol{w}(\mu), \mu\big)$
- Equilibrium $\boldsymbol{w}_0$ given by $\Rightarrow$ $\boldsymbol{R}\big(\boldsymbol{w}_0(\mu), \mu\big) = 0$
- Stability determined by eigenvalues $\lambda_j = \gamma_j \pm i\omega_j$ of Jacobian $\Rightarrow$ $A(\boldsymbol{w}_0, \mu) = \dfrac{\partial \boldsymbol{R}}{\partial \boldsymbol{w}}$
- Extended eigenvalue problem $\Rightarrow$ $\boldsymbol{R}_{EV}(\lambda, \boldsymbol{p}) = \begin{bmatrix} (A - \lambda I)\,\boldsymbol{p} \\ \boldsymbol{q}_s^T \boldsymbol{p} - i \end{bmatrix} = 0$
- BIFOR solver used for two tasks
  - Tracking of aeroelastic modes $\Rightarrow$ $\lambda_j = \lambda_j(\mu) = \gamma_j \pm i\omega_j$
  - Detecting of instability point $\Rightarrow$ $\lambda_j = \pm i\omega_j$ for $\mu = \mu^*$

[Woodgate et al, AIAA Journal 45 (2007) no. 6, pp. 1370–1381]

- Benchmark case of Isogai, NACA 64A010 aerofoil at zero angle of attack

Highly–resolved transonic instability boundary

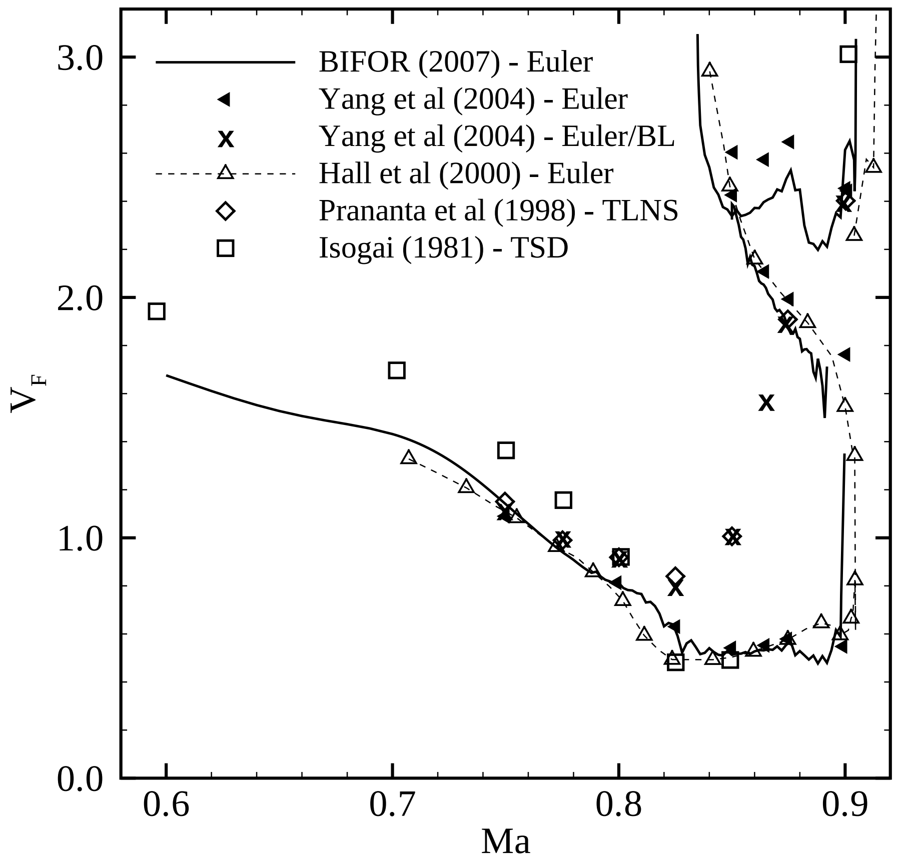

Instability boundary

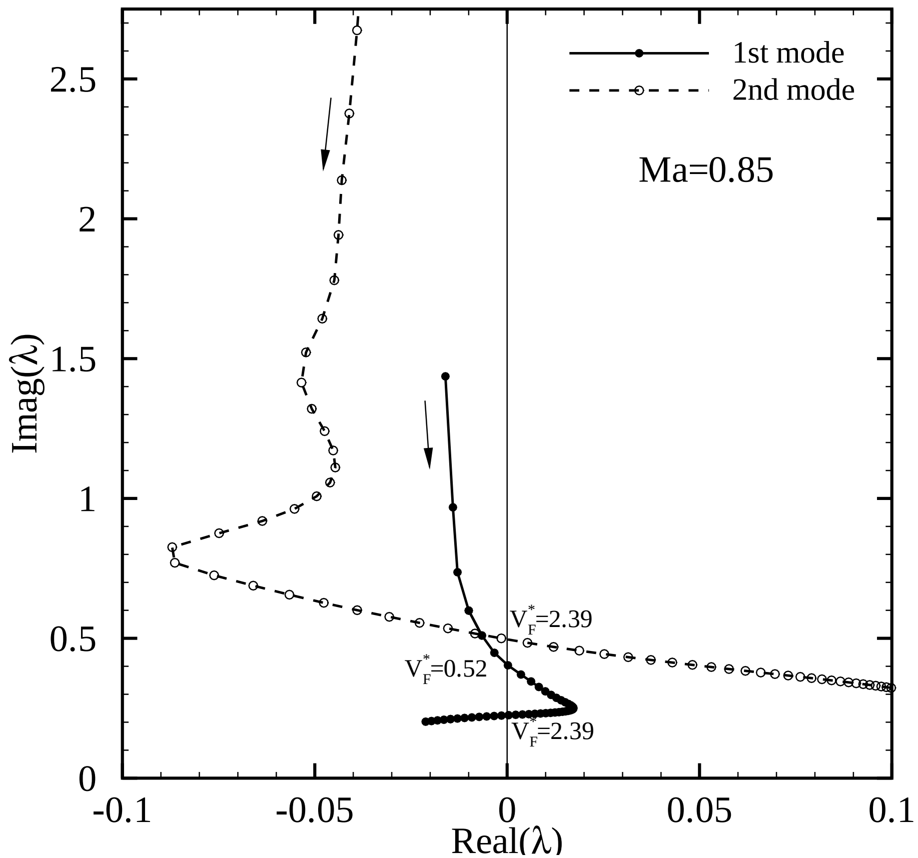

Root loci

Computational costs

Grid dimension	Steady state solver (CFL=100, conv.=1.e-10)	Eigenvalue solver (γ_j=1.e-07)	Unsteady solver (Δt=0.05, N_{step}=6.e+06)
129 x 33 (4.2k)	6 s	70 s	7 h
257 x 65 (16.7k)	60 s	600 s	30 h
513 x 65 (33.3k)	250 s	1700 s	–

Oscillatory Instability Boundary

Oscillatory Instability Boundary

- Oscillatory behaviour observed for transonic flow condition (Ma>Ma*)

NACA 0012

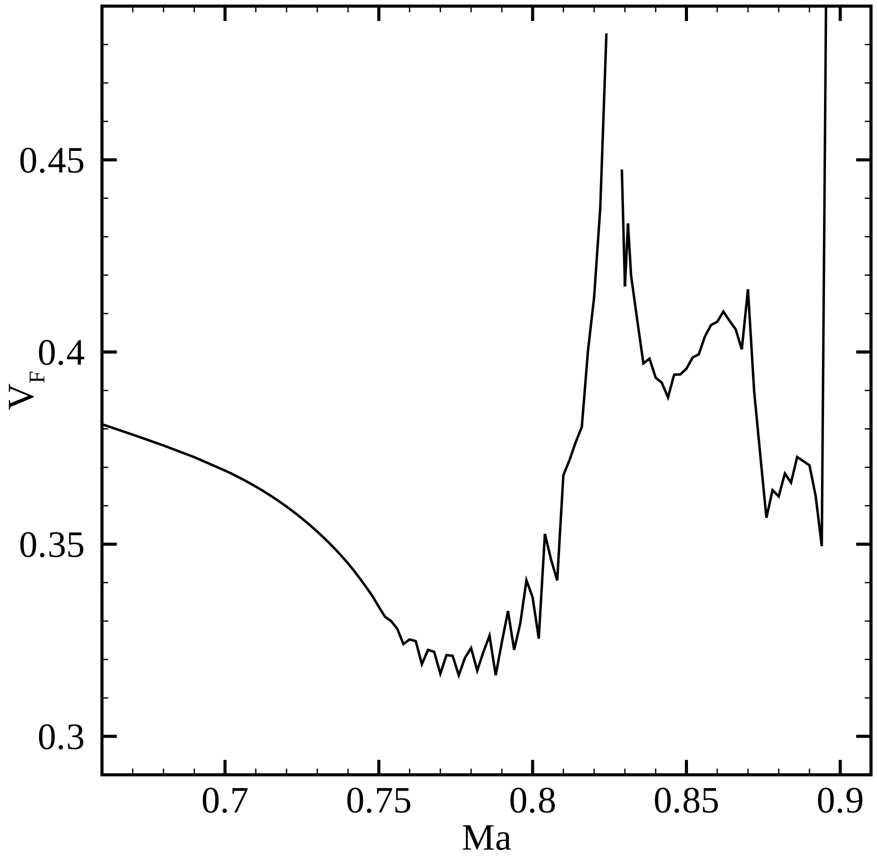

Instability boundary

Structural parameter

- aerofoil–to–fluid–mass ratio $\mu_s=100$
- ratio of natural frequencies $\omega_r=0.343$
- radius of gyration $r_\alpha=0.539$
- center of gravity $x_{cg}=0.5$
- static unbalance $x_\alpha=-0.2$

[Badcock et al, AIAA Journal 42 (2004) no. 5, pp. 883–892]

Oscillatory Instability Boundary

- NACA 0012 at zero angle of attack

3 block, C–type grid

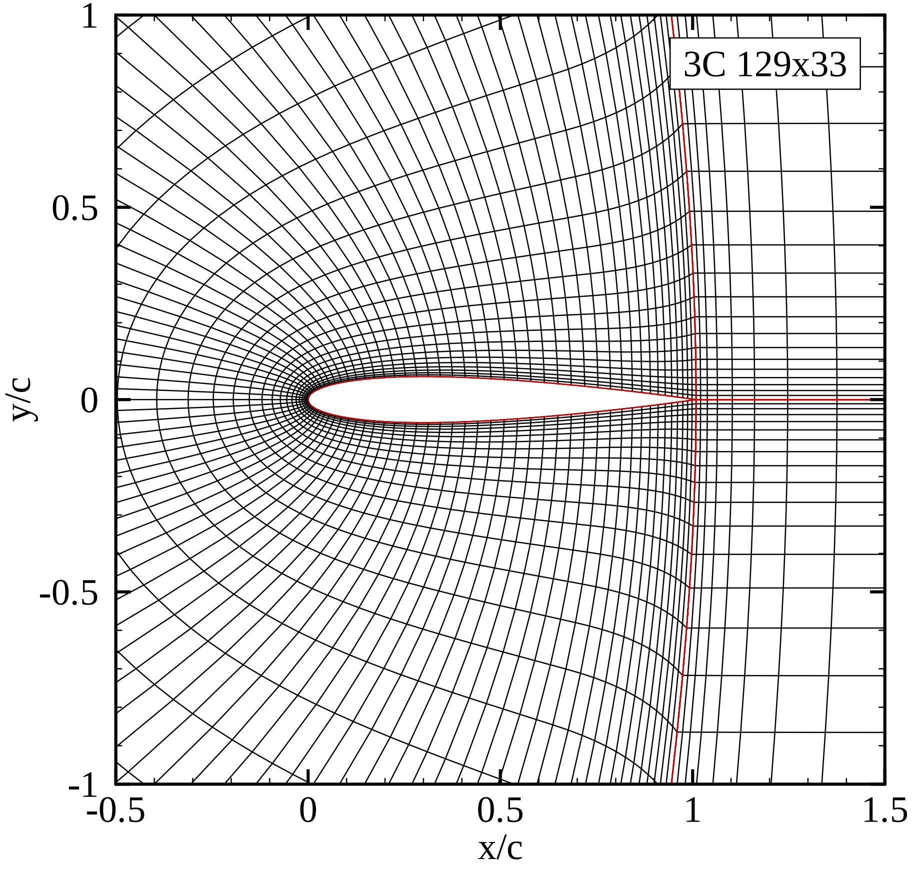

Grid topology

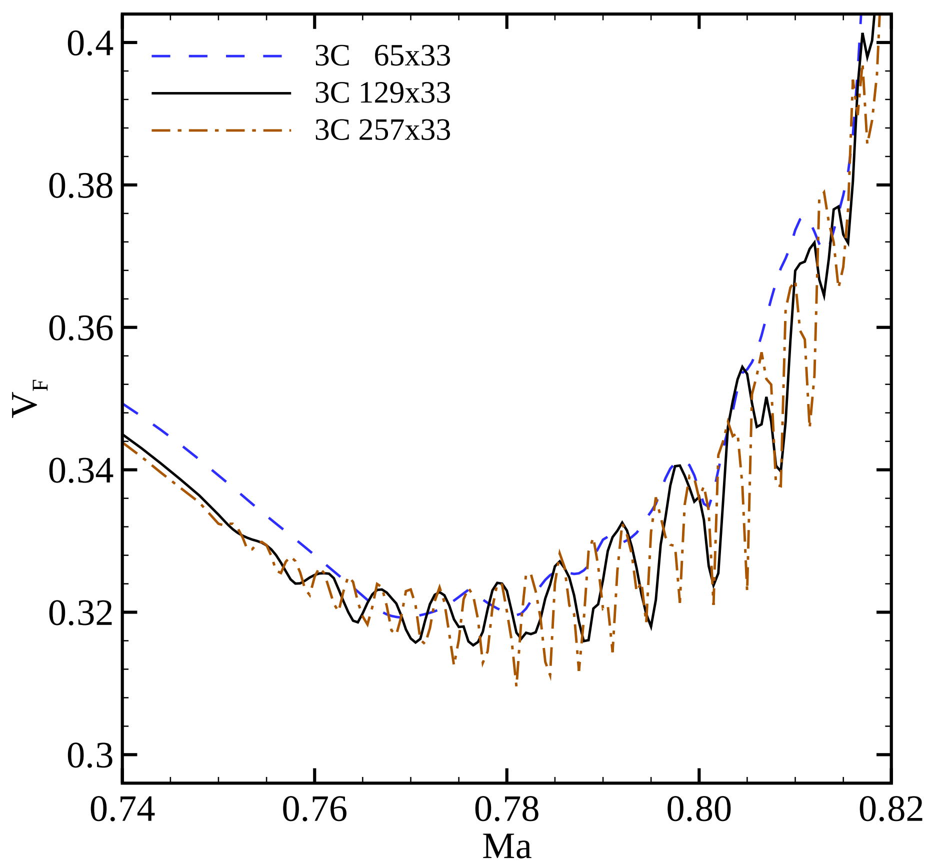

Instability boundary

Oscillatory Instability Boundary

- NACA 0012 at zero angle of attack

3 block, C–type grid

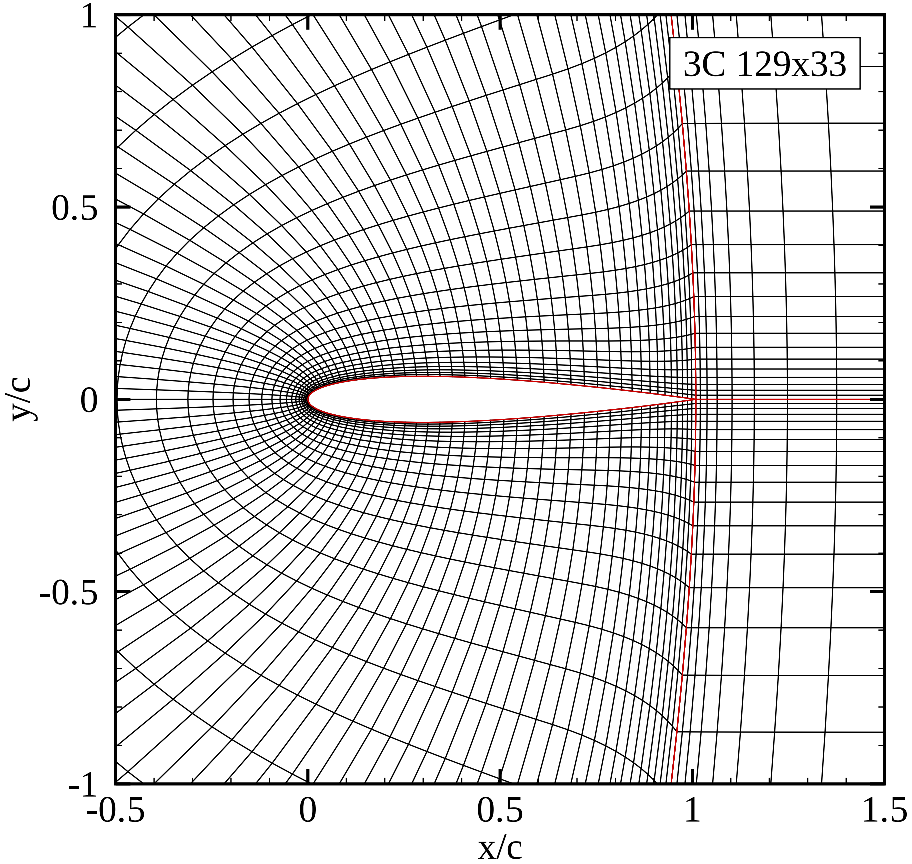

Grid topology

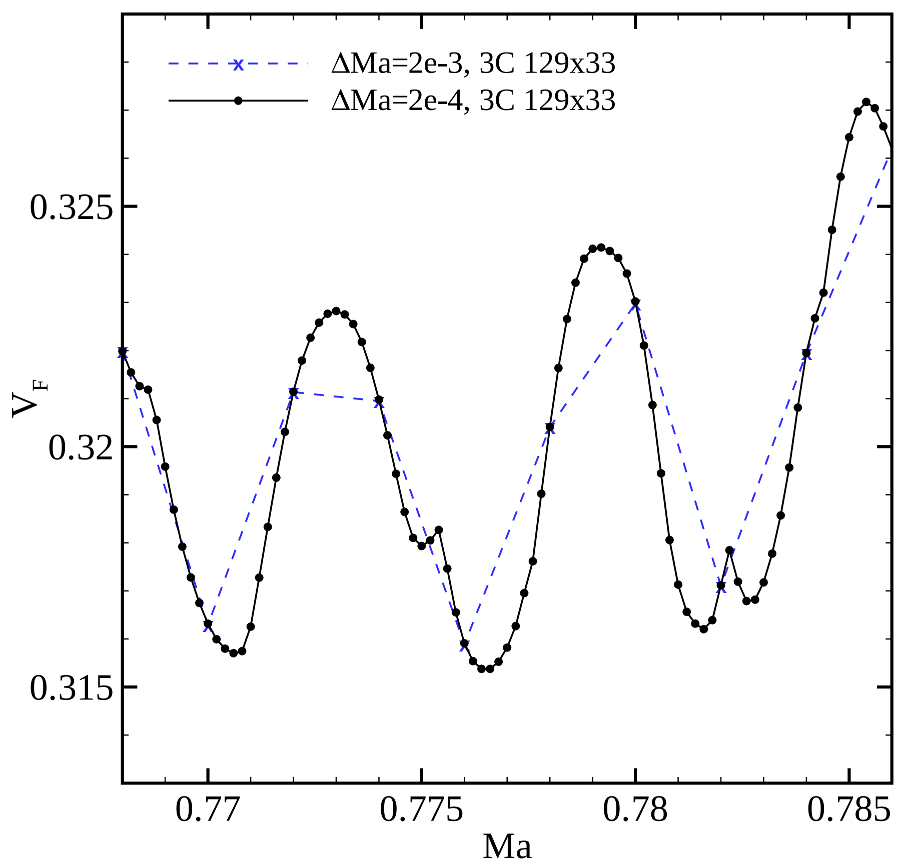

Instability boundary

Oscillatory Instability Boundary

- NACA 00xx at zero angle of attack

3 block, C–type grid

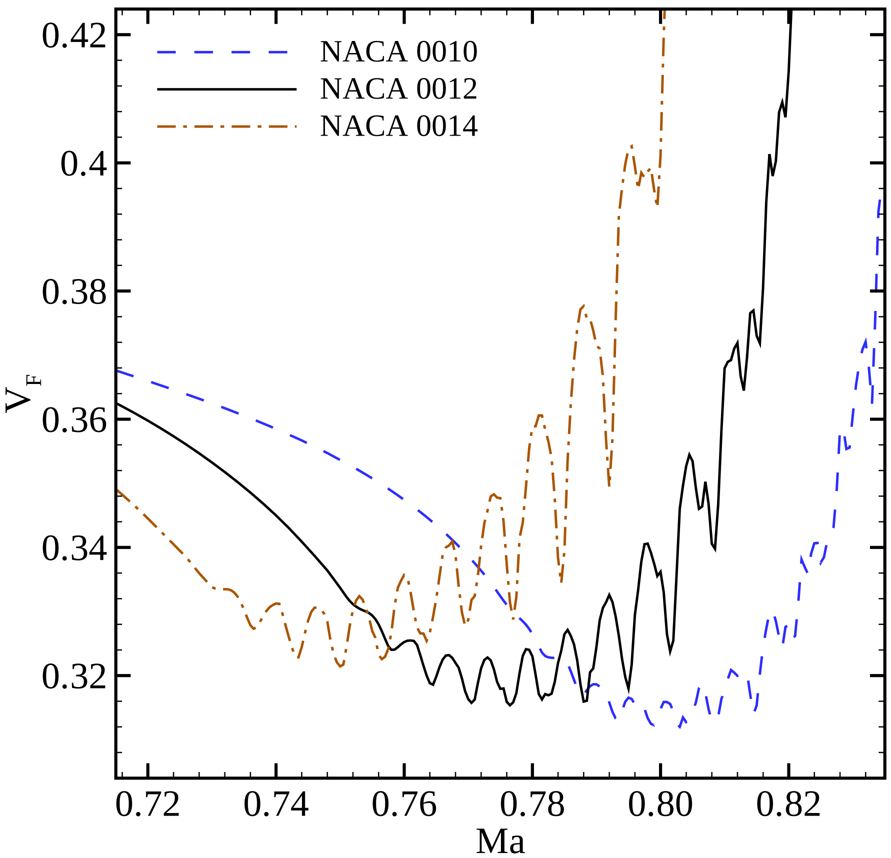

Grid topology

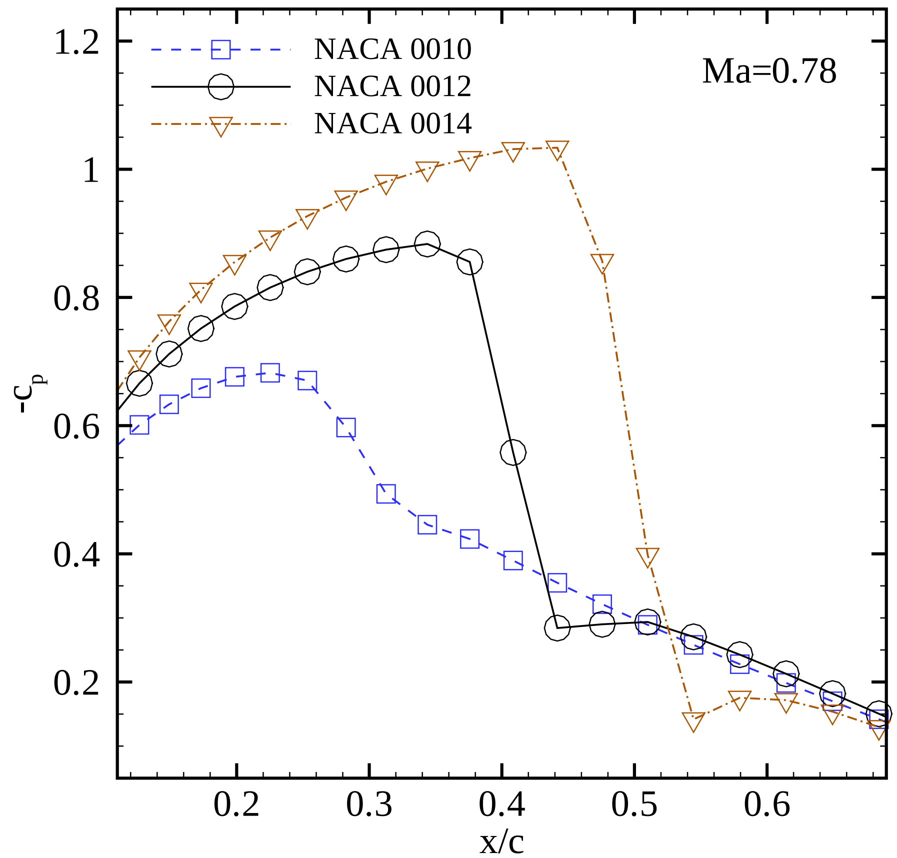

Instability boundary

Oscillatory Instability Boundary

➢ Time–accurate results crossplotted with bifurcation results

- Time–response due to initial disturbance
- Plunge rate disturbed by $\dot{h}_0 = 0.001U_\infty$

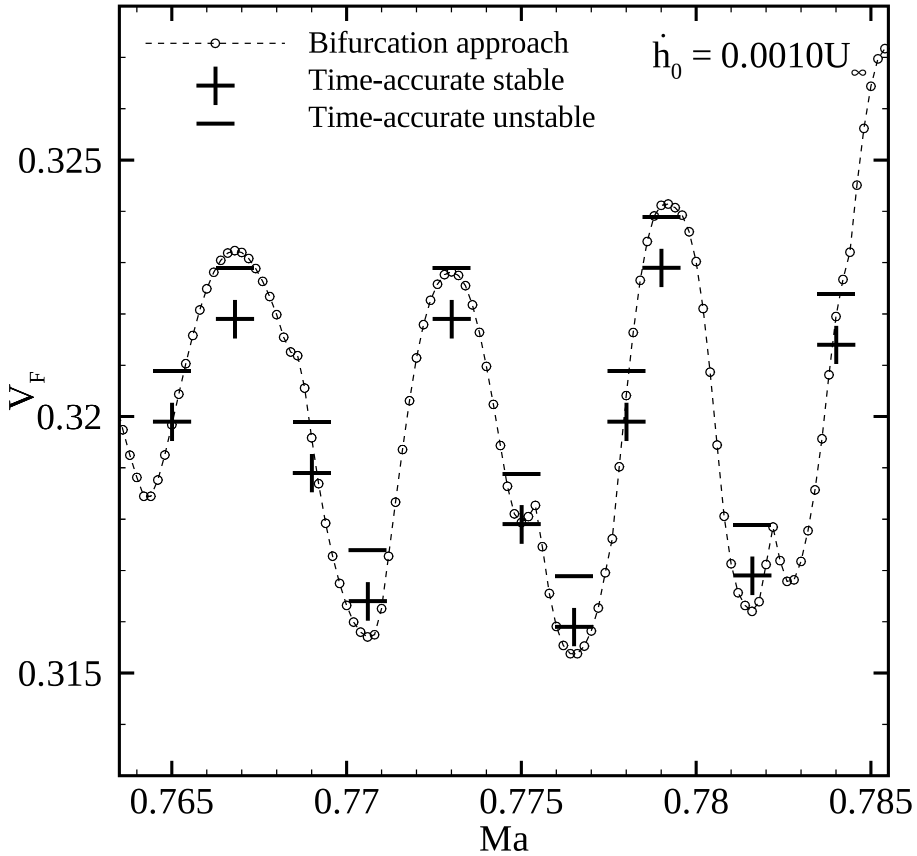

Crossplot

Oscillatory Instability Boundary

➢ Resolution of shock wave

Shock wave physically

- Event of very limited spatial extent
- Thickness of normal shock front of order

$$\delta x \approx 5.E{-}08c$$

[Granger, *Fluid Mechanics*, Holt, Rinehart & Winston]

Shock wave numerically

- Resolved thickness dependent on grid spacing

$$\Delta x_{\text{grid}} \approx 1.E{-}02c$$

- Two grids points best possible

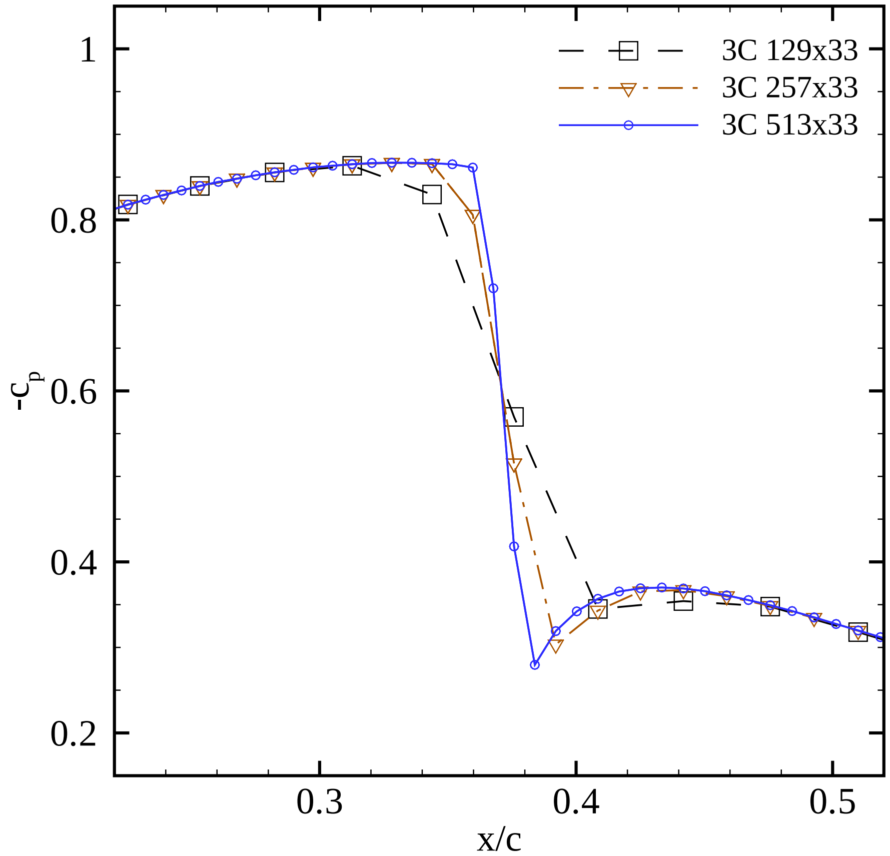

Pressure coefficient (Ma=0.773)

Oscillatory Instability Boundary

- Resolution of shock wave

Steady state results at two Mach numbers (3C 129x33)

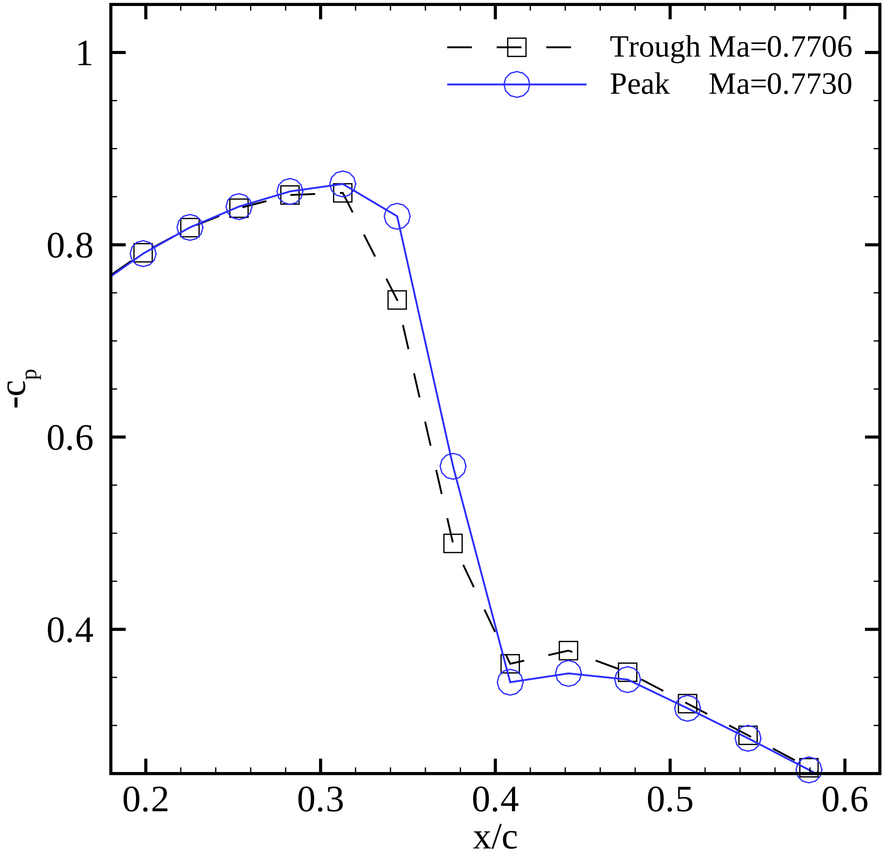

Pressure coefficient c_p

Oscillatory Instability Boundary

- Resolution of shock wave

Steady state results at two Mach numbers (3C 129x33)

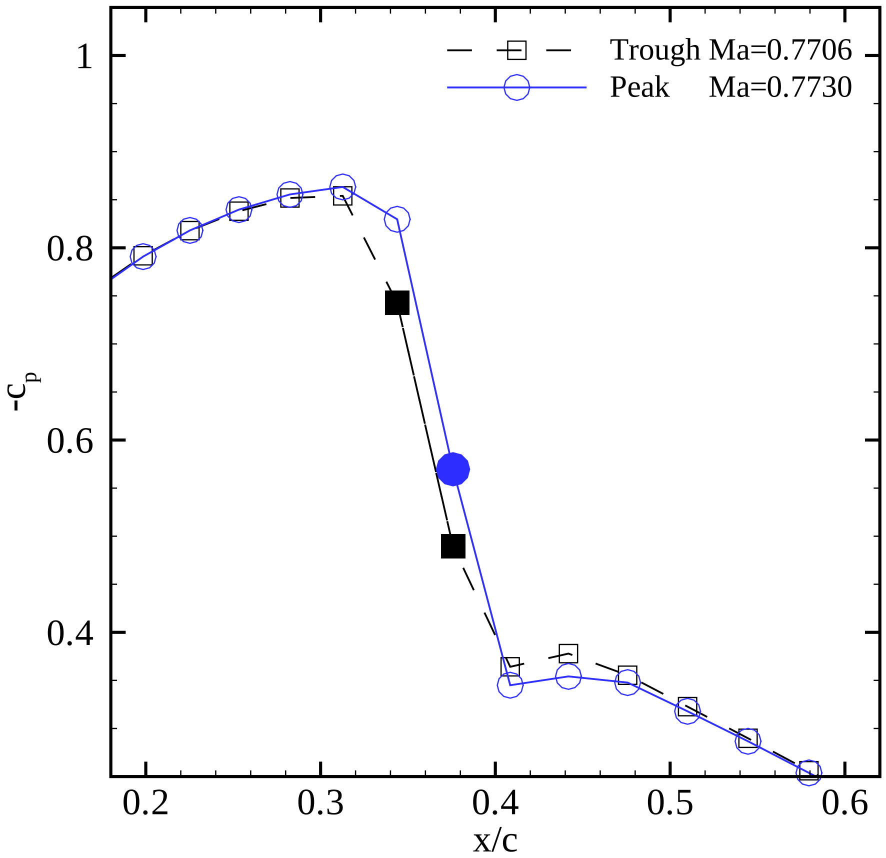

Pressure coefficient c_p

Oscillatory Instability Boundary

- Resolution of shock wave

Steady state results at two Mach numbers (3C 129x33)

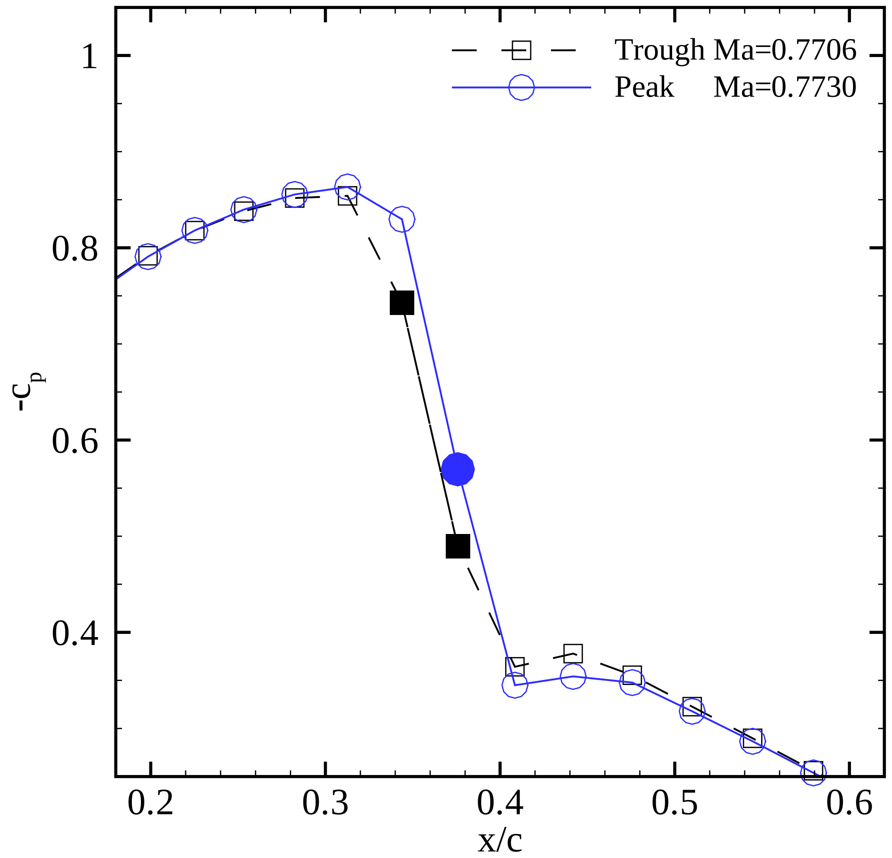

Pressure coefficient c_p

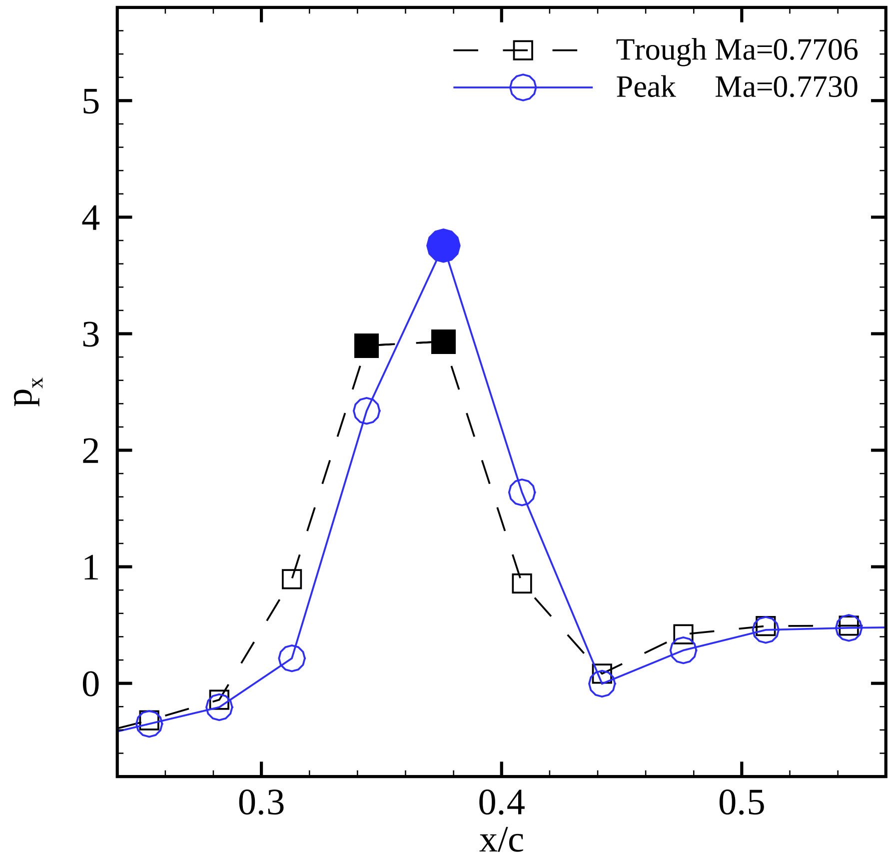

Pressure change $\partial p/\partial x$

Oscillatory Instability Boundary

- Resolution of shock wave

Steady state results at four Mach numbers (3C 129x33)

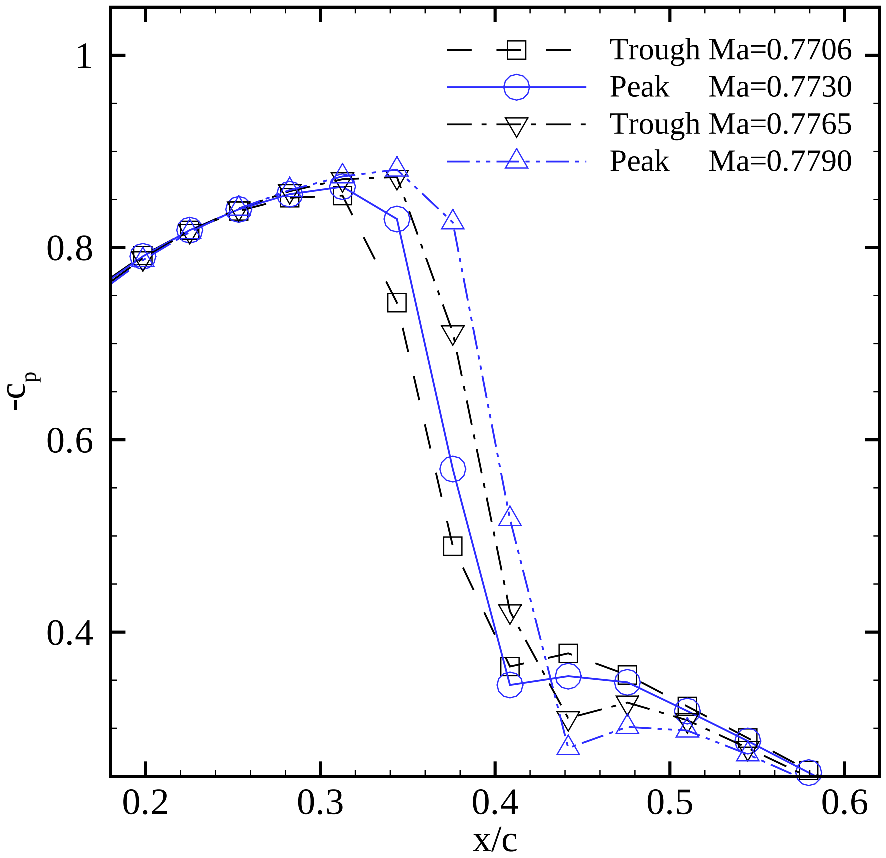

Pressure coefficient c_p

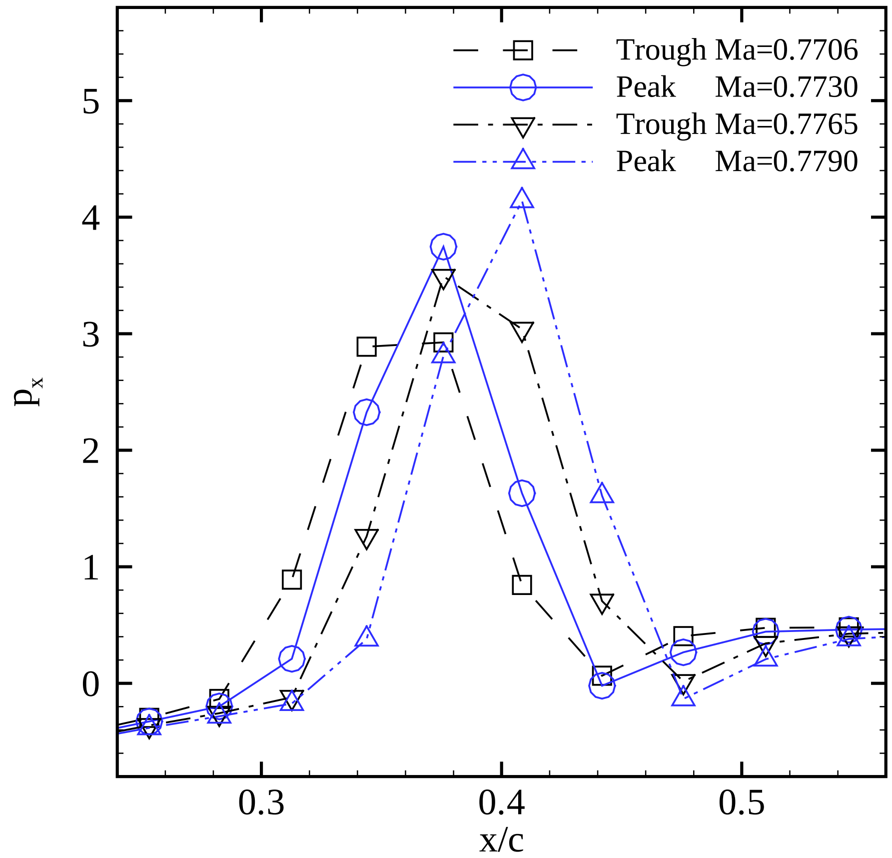

Pressure change $\partial p/\partial x$

Oscillatory Instability Boundary

- Resolution of shock wave

Steady state results at three Mach numbers (3C 129x33)

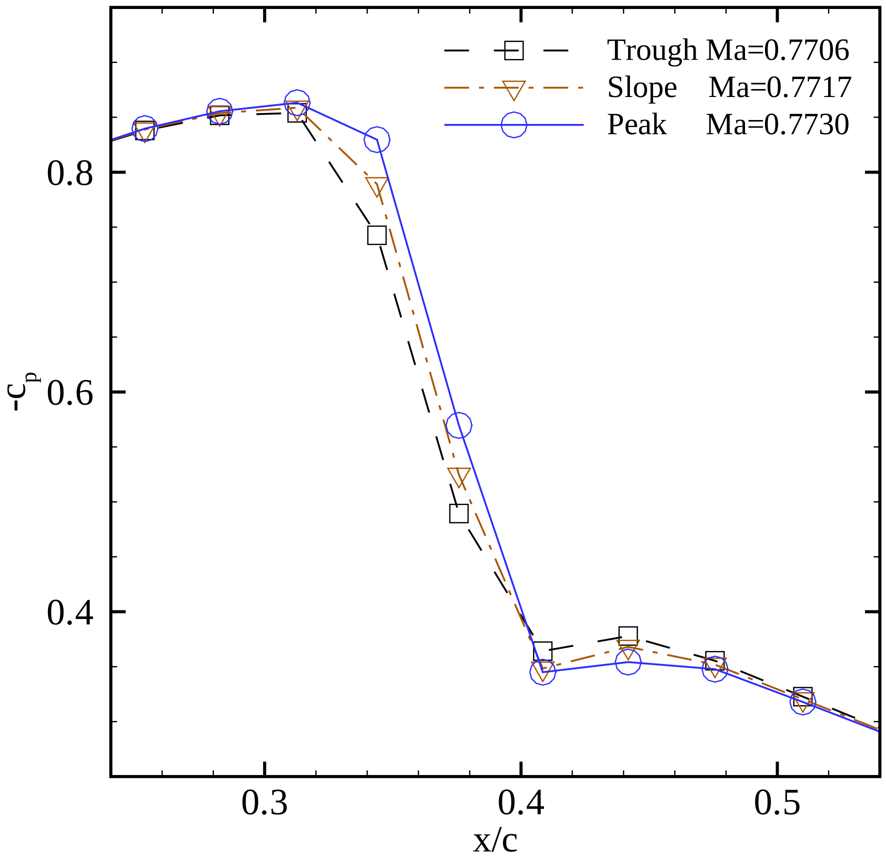

Pressure coefficient c_p

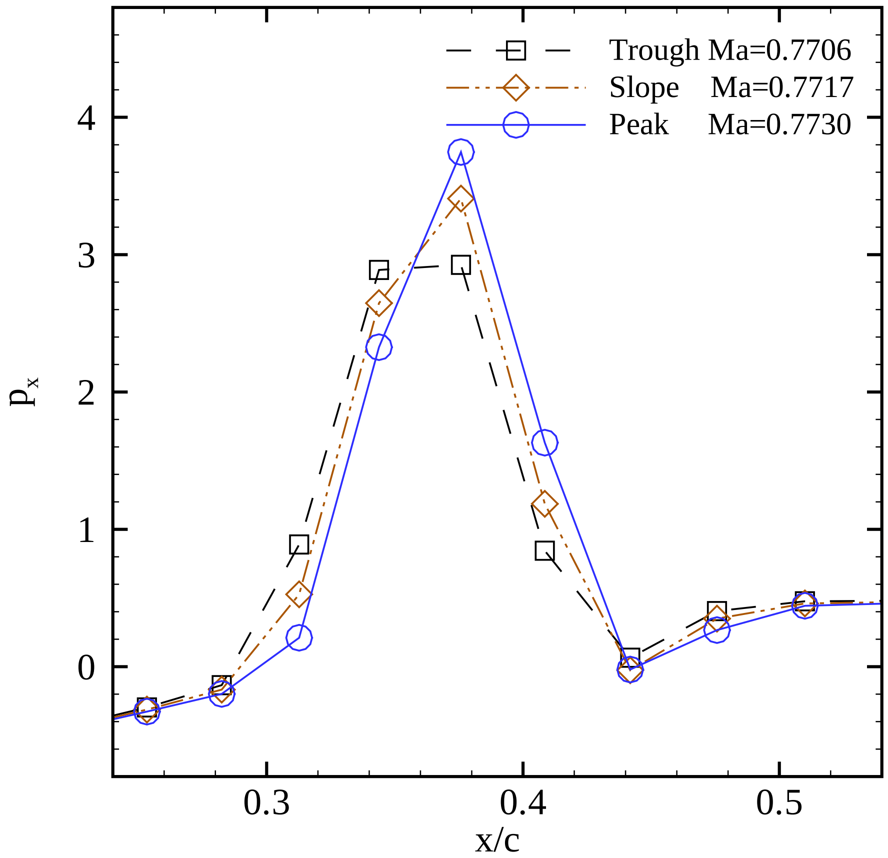

Pressure change $\partial p/\partial x$

Oscillatory Instability Boundary

- Resolution of shock wave perceived in flow field

Crossplots of instability boundary and steady state results (3C 129x33)

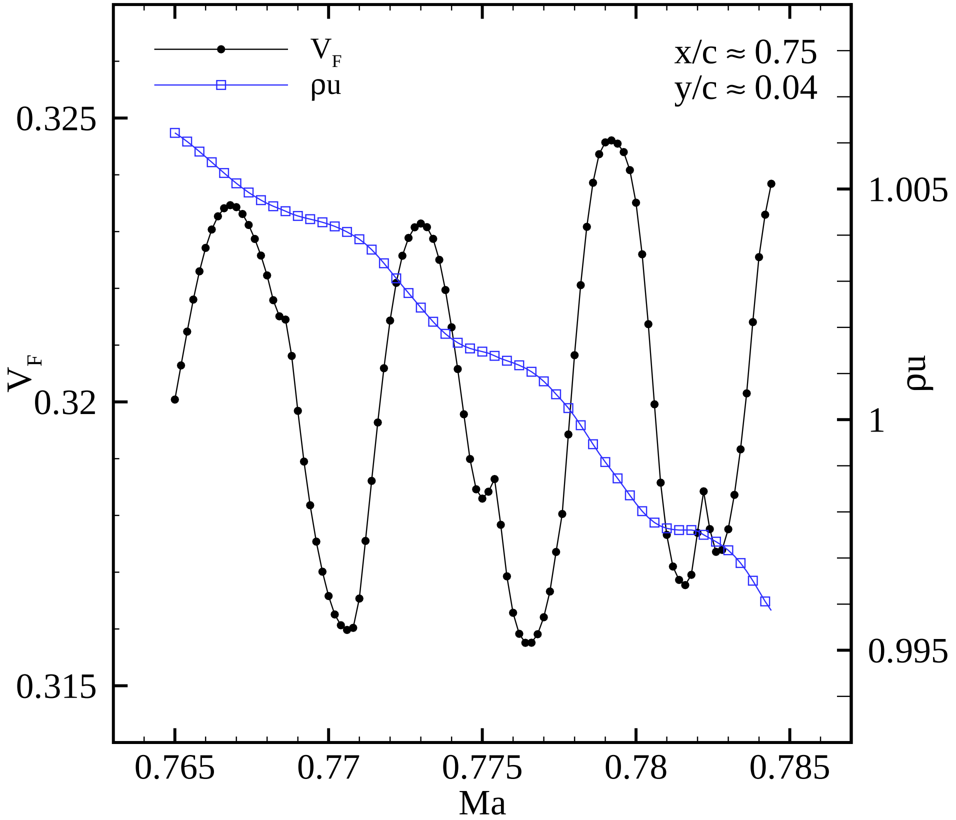

Aerofoil location (x/c≈0.75, y/c≈0.04)

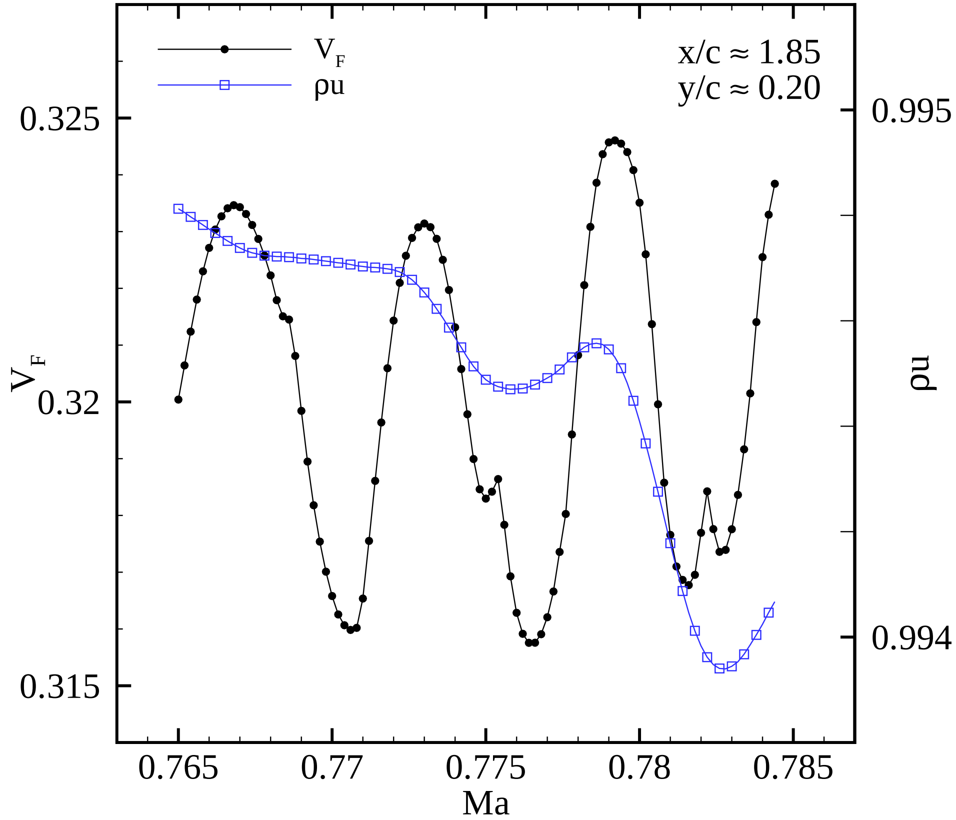

Wake location (x/c≈1.85, y/c≈0.20)

Oscillatory Instability Boundary

- Resolution of shock wave perceived in flow field

Crossplots of instability boundary and lift coefficient

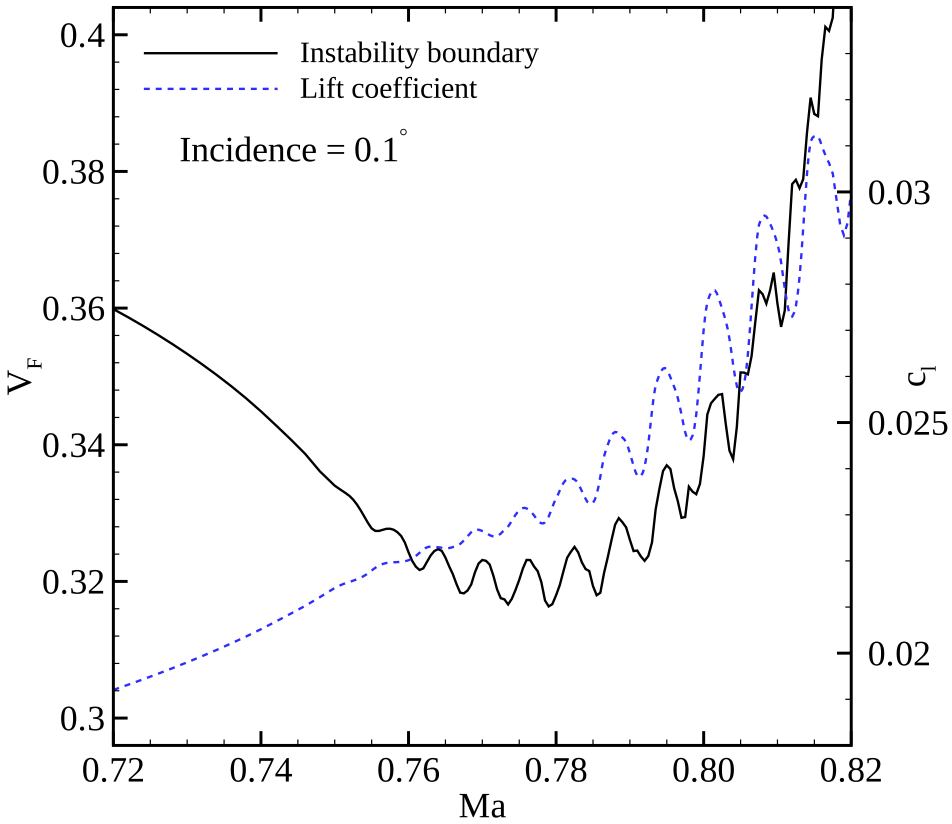

3C 129x33

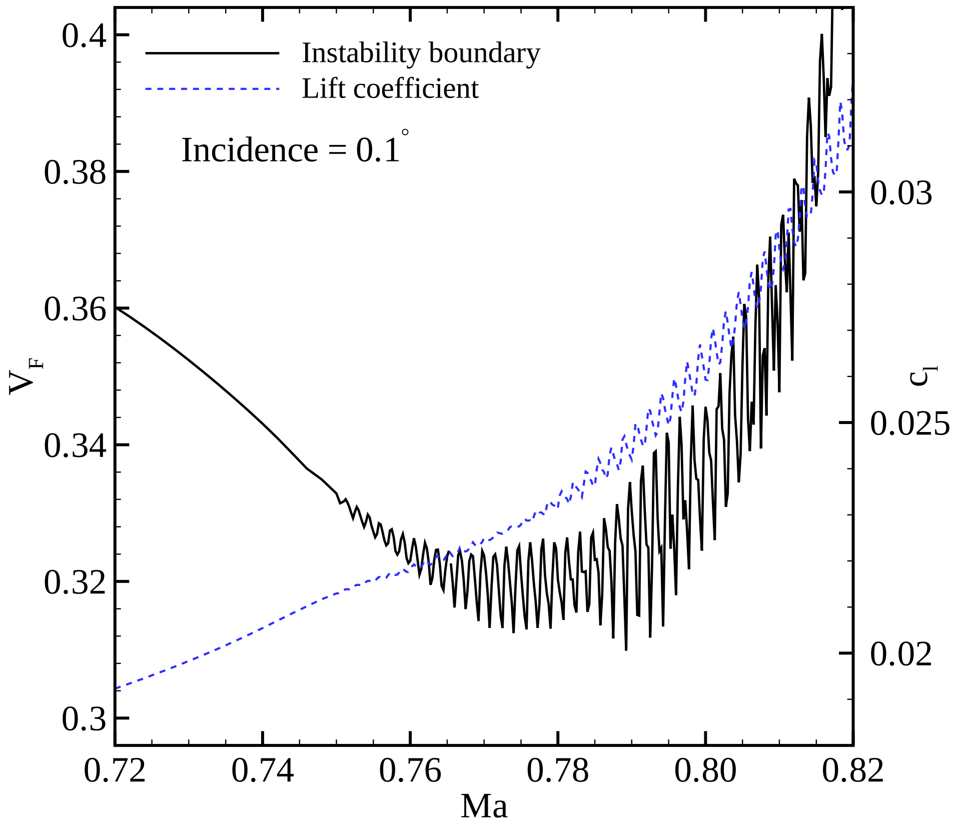

3C 513x33

Conclusion

Conclusion

- Bifurcation method using full–order nonlinear aerodynamics
- Efficient simulation of aeroelastic instabilities

Conclusion

UNIVERSITY OF LIVERPOOL

- Bifurcation method using full–order nonlinear aerodynamics
- Efficient simulation of aeroelastic instabilities

* * *

- High resolution of instability boundary revealed oscillatory behaviour
- Numerical artefact due to shock wave resolution

ECERTA PROJECT

Computational Aeroelasticity
based on
Bifurcation Theory

Sebastian Timme
sebastian.timme@liverpool.ac.uk

Kenneth J. Badcock
k.j.badcock@liverpool.ac.uk

UNIVERSITY OF
LIVERPOOL